EJNMMI Radiopharmacy and Chemistry

RESEARCH ARTICLE Open Access

Sustainable production of radionuclidically pure antimony-119

Aeli P. Olson[1], Francesca A. Verich[1], Paul A. Ellison[1], Eduardo Aluicio-Sarduy[1], Robert J. Nickles[1], Jason C. Mixdorf[1], Todd E. Barnhart[1] and Jonathan W. Engle[1,2*]

*Correspondence:
Jonathan W. Engle
jwengle@wisc.edu
[1]Department of Medical Physics, University of Wisconsin, Madison, WI 53705, USA
[2]Department of Radiology, University of Wisconsin, Madison, WI 53705, USA

Abstract

Background Radiopharmaceutical therapy (RPT) uses radionuclides that decay via one of three therapeutically relevant decay modes (alpha, beta, and internal conversion (IC) / Auger electron (AE) emission) to deliver short range, highly damaging radiation inside of diseased cells, maintaining localized dose distribution and sparing healthy cells. Antimony-119 (^{119}Sb, $t_{1/2}$ = 38.19 h, EC = 100%) is one such IC/AE emitting radionuclide, previously limited to in silico computational investigation due to barriers in production, chemical separation, and chelation. A theranostic (therapeutic/diagnostic) pair can be formed with ^{119}Sb's radioisotopic imaging analogue ^{117}Sb ($t_{1/2}$ = 2.80 h, E_γ = 158.6 keV, I_γ = 85.9%, β^+ = 262.4 keV, $I_{\beta+}$ = 1.81%).

Results Within, we report techniques for sustainable and cost-effective production of pre-clinical quality and quantity, radionuclidically pure ^{119}Sb and ^{117}Sb, novel low energy photon measurement techniques for ^{119}Sb activity determination, and physical yields for various tin target isotopic enrichments and thicknesses using (p, n) and (d, n) nuclear reactions. Additionally, we present a two-column separation providing a radioantimony yield of 73.1% ± 6.9% (N = 3) and tin separation factor of (6.8 ± 5.5) x 10^5 (N = 3). Apparent molar activity measurements for deuteron produced ^{117}Sb using the chelator TREN-CAM were measured at 42.4 ± 25 MBq ^{117}Sb/μmol (1.14 ± 0.68 mCi/μmol), and we recovered enriched ^{119}Sn target material at a recycling efficiency of 80.2% ± 5.5% (N = 6) with losses of 11.6 mg ± 0.8 mg (N = 6) per production.

Conclusion We report significant steps in overcoming barriers in ^{119}Sb production, chemical isolation and purification, enriched target material recycling, and chelation, helping promote accessibility and application of this promising therapeutic radionuclide. We describe a method for ^{119}Sb activity measurement using its low energy gamma (23.87 keV), negating the need for attenuation correction. Finally, we report the largest yet-measured ^{119}Sb production yields using proton and deuteron irradiation of natural and enriched targets and radioisotopic purity > 99.8% at end of purification.

Introduction

In radiopharmaceutical therapy (RPT), a radionuclide with medically relevant decay properties is incorporated into a molecular construct that targets a physiological disease pathway. RPT can be coupled with surgery, chemotherapy, immunotherapy, and potentially other technologies, and consists of components which can be tailored to application: a radiometal, a bifunctional chelator, linker, and a targeting moiety (Bodei et al. 2023).

Therapeutic radionuclides decay via one of four relevant processes: alpha, beta, electron capture, and internal conversion (IC). Additionally, Auger electron (AE) emission(s) can be initiated after electron capture and IC decays. For conversion and Auger electron (IC/AE) emitting radionuclides, ideal properties include high IC and AE yield, minimal photon co-emission, half-life suitably long enough for production and distribution, and widely available chemical separation and chelation strategies (Bolcaen et al. 2023). Antimony-119 (^{119}Sb, $t_{1/2}$ = 38.19 h, EC=100%) (Symochko et al. 2009) garners attention as a potential therapeutic radionuclide due to the high linear energy transfer of its 23–24 Auger and conversion electrons (Eckerman and Endo 2008). Based on these studies (Bernhardt et al. 2001; Bolcaen et al. 2023; Falzone et al. 2015; Filosofov et al. 2021; Ku et al. 2019; Thisgaard and Jensen 2008), ^{119}Sb is considered a promising AE emitting radionuclide due primarily to high IC/AE yield, high cellular dosimetry S-values, and few co-emitted gammas (Bolcaen et al. 2023), and ^{119}Sb forms a theranostic pair with the radioisotopic imaging analogue ^{117}Sb (^{117}Sb, $t_{1/2}$ = 2.80 h, E_{γ}=158.6 keV, I_{γ}=85.9%, $E_{\beta+\text{mean}}$ = 262.4 keV, $I_{\beta+}$ = 1.81%) (Blachot 2002). Historically, ^{119}Sb dosimetry has been limited to in silico study due to barriers in production and chemical coordination. Production of ^{119}Sb has previously been reported once, via proton bombardment of 97.4% isotopically enriched ^{119}Sn at a target thickness of 5.5 mg/cm^2 (^{119}Sn(p, n)^{119}Sb nuclear reaction), measuring an end of bombardment (EOB) physical yield of 1.85 MBq/μAh (Thisgaard and Jensen 2008). The same research group recycled (75% Sn recovery) ^{nat}Sn by electrodeposition from basic solution, creating targets with a maximum areal density of 15 mg/cm^2 (Thisgaard and Jensen 2009). Using a high-power 6° slant target geometry, similar thickness ^{nat}Sn targets withstood 150 μA of 13 MeV proton beam current (Thisgaard et al. 2011).

Clinical production of radionuclidically pure ^{119}Sb is scalable via the ^{119}Sn(p, n)^{119}Sb or ^{118}Sn(d, n)^{119}Sb nuclear reactions which requires recycling of enriched $^{118/119}$Sn. Various chemical separation techniques to remove bulk tin target material and isolate radioantimony have been reported (Kostelnik et al. 2023; Randhawa et al. 2021), but bifunctional chelation of purified radioantimony has not been reported. Direct coordination of radioantimony from an unseparated, dissolved target solution has been reported (Olson et al. 2021), but concentrated HCl conditions are too harsh for labeling with biologically targeted complexes. Complexation and in vivo stability characterization of tricatecholate TREN-CAM (Joaqui-Joaqui et al. 2020; Koller et al. 2024; Olson et al. submitted 2024) with radioantimony produced via liquid-liquid extraction (Kostelnik et al. 2023) has been recently reported; however, this separation technique requires manual manipulation and is harder to automate than column chromatography methods, which reduce user dose. Existing column chromatography-based separations employ cation or anion exchange resins and oxidants (H_2O_2) to primarily separate Sn^{4+} and Sb^{5+}. These techniques generally require large elution volumes and provide radioantimony and tin target

material in solvent matrices and speciation unideal or incompatible with chelation and target recycling strategies (Grundmane et al. 2024; Randhawa et al. 2021). The thiophilic quality of pnictogens motivated exploration of a thiol functionalized resin for radioantimony purification reported here.

Materials and methods

Chemicals

Bombardment of tin with protons or deuterons produces radioactive isotopes of antimony and tin, with emissions including gammas, X-rays, positrons, and electrons. Proper radiation safety shielding and handling techniques are necessary for experiments with radioactive material. All radiation work was conducted with safe technique in lab spaces approved for radionuclide application.

All reagents and starting materials were purchased from commercial vendors and used without further purification. All solutions were prepared with 18 MΩ*cm deionized water (MilliQ water). Concentrated hydrochloric acid (c.HCl), sodium hydroxide (NaOH), and ethanol (EtOH) were sourced from Fisher Chemicals (Hampton, NH, USA). Methanol (MeOH) and normal phase silica TLC plates were purchased from Sigma-Aldrich (Burlington, MA, USA). VWR Life Sciences (Radnor, PA, USA) supplied dimethyl sulfoxide (DMSO), and EMD Chemicals (Gibbstown, NJ, USA) supplied ammonium acetate (NH_4OAc).

Electroplating tin cyclotron targets

The sulfuric acid-based plating solution and electrodeposition parameters were reported previously for creation of 100 mg ^{nat}Sn targets (Olson et al. 2021). $SnSO_4$ was sourced from Strem Chemicals (Newburyport, MA, USA). These parameters plate ~ 50 mg metallic Sn per mL electrolyte, and for larger mass targets, larger electrolyte volumes were used. In creation of isotopically enriched ^{119}Sn (Table 1, Isoflex, San Francisco, CA, USA) targets, metal foil purchased in 2018 for 6 USD/mg was dissolved in c.HCl at room temperature and reclaimed using recycling techniques described below.

Target irradiation and activity characterization

Metallic tin targets (8 mm ⌀, 80–760 mg/cm^2, see Table 1) were electroplated as described above upon gold and silver target backings. A GE PETtrace cyclotron was used to irradiate Sn targets with up to 16 MeV protons and 8 MeV deuterons. A 500 µm thick aluminum degrader reduced incident 16 MeV beam energy down to 12.5 MeV. To

Table 1 Composition of irradiated natural and isotopically enriched ^{119}Sn targets

Stable Tin Isotopes	Natural Enrichment	Isotopically Enriched
Sn-112	0.97	0.001
Sn-114	0.66	0.001
Sn-115	0.34	0.006
Sn-116	14.54	0.014
Sn-117	7.68	0.019
Sn-118	24.22	2.57
Sn-119	8.59	96.3
Sn-120	32.58	1.056
Sn-122	4.67	0.019
Sn-124	5.79	0.016

minimize unnecessary dose to radiation workers, proton irradiated targets were decayed overnight before use. Deuteron irradiated targets were decayed a minimum of 45 min before retrieval.

End of bombardment (EOB)-corrected physical yields(Otuka and Takács 2015) for ^{117}Sb, ^{118m}Sb, ^{120m}Sb, ^{122}Sb, ^{124}Sb, and ^{125}Sb were quantified via gamma spectroscopy with an aluminum-windowed high purity germanium (HPGe) detector (AMETEK ORTEC, Knoxville, Tennessee) coupled to a Canberra (Concord, Ontario) Model 2025 research amplifier and multichannel analyzer calibrated with ^{241}Am, ^{133}Ba, ^{152}Eu, ^{137}Cs, and ^{60}Co sources (Amersham PLC, Little Chalfont, U.K.) for energy and efficiency. The system has a full width at half-maximum resolution of 1.8 keV at 1333 keV. Antimony-117 ($t_{1/2}$ = 2.80 h) and ^{117m}Sn ($t_{1/2}$ = 14 d) share a 158.56 keV photon emission. After ^{117}Sb decayed (>30 h post EOB), ^{117m}Sn activities were quantified and ^{117}Sb yields corrected for ^{117m}Sn signal contribution. Measured EOB corrected physical yields were compared against theoretically predicted yields from the IAEA medical isotope browser and TENDL sourced cross-sections (IAEA 2024). Radioisotopic purity is reported as the percent activity of choice radioisotope within the sum of all radioactive isotopes.

Antimony-119 yields were measured using a Be-windowed cadmium telluride (CdTe, Amptek X-123) X-ray spectrometer calibrated for energy and efficiency using ^{241}Am, ^{133}Ba, and ^{152}Eu check sources. Quantifying ^{119}Sb activity in solution or solid, undissolved targets is challenging because of high susceptibility to attenuation and scatter of its sole, low-energy gamma (E_γ=23.87 keV, I_γ=16.5%). To obviate the need for attenuation correction, massless sources were made for spectrometry (Scheme 1) and mounted perpendicular to the benchtop and in line with the CdTe detector face, preventing the walls of the plastic microcentrifuge tubes from impeding detected photons. In this application, the term 'massless source' is describing a radioactive source in which liquid and solid mass have been removed, ensuring no material is impeding and attenuating low energy ^{119}Sb photon emissions before CdTe detection. After target dissolution and radioantimony purification, 10 µL of radioantimony was reserved in a microcentrifuge vial and dried overnight to form a massless source. These dried, uncovered aliquots of purified radioantimony were mounted in line with the CdTe detector face (Scheme 1 right). To accurately quantify ^{119}Sb yields, the same massless sources were assayed on

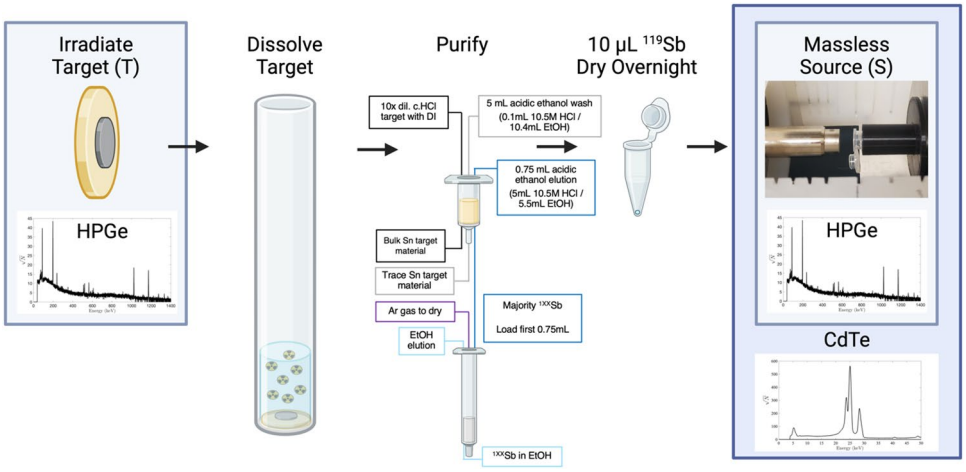

Scheme 1 Illustration of ^{119}Sb massless source creation, spectra collection, and irradiated target yield correction workflow. Created in BioRender. Olson, A. (2024) http://www.BioRender.com/h73h197

both the HPGe and CdTe detectors. The total activity ^{119}Sb activity (T_{119Sb}) in the target was calculated using ^{120m}Sb as a tracer, measuring the fraction of ^{120m}Sb from the total target activity (T_{120mSb}) in the massless source ((S_{120mSb}) to correct the measured massless source ^{119}Sb activity (S_{119Sb}) (Eq. 1).

$$T_{119Sb} = (S_{119Sb}) \left(\frac{T_{120mSb}}{S_{120mSb}} \right) \quad (1)$$

Peak counts greater than 3000 resulted in counting uncertainties less than 2%, and yield measurement uncertainties are expressed as the standard deviation of N=3 replicate productions.

Radiochemical isolation of radioantimony from bulk target material

Irradiated targets were dissolved in 6 mL c.HCl at 90 °C for 1–2 h in a glass tube under N_2, after which the dissolved target solution was removed from heated glass chamber, and the inside of the chamber was washed with 2 mL c.HCl, creating a combined volume of 8 mL. Antimony was chemically separated from ^{nat}Sn or ^{119}Sn target material using two sequential chromatographic columns—a 100 mg mercaptopropyl functionalized silica gel resin (Sigma-Aldrich, 200–400 mesh) packed in a 8.8 mm ID column (Sigma-Aldrich, 20 µm top and bottom frits) preconditioned with 10 mL 1 M HCl, 10 mL 0.1 M HCl, and 10 mL H_2O and a second 100 mg Prefilter resin (Eichrom, 100–150 mesh) packed column with 5.5 mm ID (Sigma-Aldrich, 20 µm top and bottom frits) preconditioned with 10 mL EtOH then 10 mL MilliQ water. The dissolved target solution was diluted 10X with MilliQ water and loaded onto mercaptopropyl resin. Loaded resin was washed with 5 mL 99% EtOH, 0.1 M HCl prepared by combining 0.1 mL 10.5 M HCl with 10.4 mL EtOH. Antimony eluted from the resin using 1.5 mL 48% EtOH, 5 M HCl prepared by combining 5 mL 10.5 M HCl with 5.5 mL EtOH fractionated into two 750 µL volumes. The first 750 µL fraction was loaded onto a second column comprised of Prefilter resin. Argon was passed through the loaded Prefilter resin to dry acidic EtOH from the column. After 40 min of column drying, 5 mL of EtOH eluted the radioantimony from the column and was used directly for radiolabeling experiments.

Chemical analysis and apparent molar activity measurement

Trace metal contamination was measured using an Agilent (Santa Clara, CA, USA) 5800 inductively coupled plasma optical emission spectrometer (ICP-OES). For measurement of samples in organic matrices, a 0.8 mm inner diameter (ID) torch replaced the standard 1.2 mm ID torch. Calibration curves were generated by diluting commercially available standards of Sn, Zn, Cu, Ni, Fe, Co purchased from Sigma-Aldrich (St. Louis, MO, USA) and Sb (SPEX CertiPrep, Metuchen, NJ, USA) with sample matching matrices to the following concentrations: 50 ppm, 10 ppm, 5 ppm, 1 ppm, 0.5 ppm, and 0.1 ppm. For transition metals, limits of detection are typically in the ppb range and ppm range for organometallic elements.

To investigate high molarity HCl decomposition of mecaptopropyl resin, eluent fraction thiol concentrations were quantified using Ellman's reagent (Ellman 1959; Riddles et al. 1983)—a UV-Vis active disulfide bond-containing compound that loses UV activity when reacted with thiols. Ellman's reagent (Sigma-Aldrich) reacts 1:1 with free thiols, therefore its 412 nm absorbance measurement is linearly related to solution thiol

concentration. Using an Ocean Optics UV-Vis spectrometer (USB-LS-450, Ocean Insight, Orlando, FL, USA) and OceanView software, a calibration curve was constructed by reacting solutions of known cysteine concentration (0.1 µM, 1 µM, 10 µM, 50 µM, 100 µM, 250 µM, and 500 µM) with 0.01 M Ellman's reagent in 0.1 M Na_2PO_4 pH 7.5. Thiol resin elution fractions were neutralized with 1 M NaOH, as highly acidic environments reduce Ellman's reagent, combined with equal volume Ellman's reagent solution, monitored for 412 nm absorbance, and compared against calibration curve for thiol concentration determination.

Apparent molar activity (AMA) quantification via titration was measured with the synthetic siderophore mimicking ligand "TREN-CAM" (Olson et al. submitted 2024) synthesized via established methods (Scheme S1). 10 µL TREN-CAM stock solution (20% DMSO in MilliQ water), 80 µL 0.5 M NH_4OAc buffer pH 6, and 10 µL chemically purified ^{117}Sb (0.7–2.5 MBq) produced via 8 MeV deuteron bombardment of ^{nat}Sn were combined at final reaction concentrations of 0.01 mM, 0.1 mM, 0.5 mM, and 1 mM TREN-CAM and heated at 80 °C for 1 h. Complexation was assessed via thin layer chromatography (TLC), spotting aliquots of radiolabeling solutions onto Al-backed Si TLC plates, and developing the plates with MeOH mobile phase separated [^{117}Sb]Sb-TREN-CAM ($R_f = 0.755 \pm 0.005$ ($N=3$)) from free ^{117}Sb ($R_f = 0.019 \pm 0.009$ ($N=3$) where uncertainties are expressed as standard deviation or measurement replicates). Autoradiography (Packard Cyclone Storage Phosphor) was used to quantify complexation and radioactive impurities. Fitting the fraction of complexed ^{117}Sb to a sigmoid curve allowed determination of moles TREN-CAM necessary to quantitatively complex reacted ^{117}Sb activity.

Recycling target material

Sn target material was recycled by combining load and wash fractions and neutralizing with NaOH, precipitating $Sn(OH)_2$. The solution was centrifuged to concentrate the $Sn(OH)_2$ precipitate into a pellet. The supernatant was twice discarded and $Sn(OH)_2$ washed with MilliQ water. Afterwards, concentrated H_2SO_4 was added to the precipitated pellet, dissolving the $Sn(OH)_2$ and forming $SnSO_4$. Additional electroplating constituents were added according to ratios in Table 2. MilliQ water diluted electrolytic solution to final total volume. The electrolyte was biased to 3 V for 48 h with a platinum anode and target backing.

Results

Electroplating tin targets for cyclotron targetry

Dense, thermally conductive ^{nat}Sn targets for proton/deuteron irradiation were created using an electrodeposition technique with strong adherence observed when electroplating upon either silver or gold target backings. Two such targets are shown in Fig. 1. The

Table 2 Ratios of electroplating constituents used to recycle target material

Component	Value
Dissolved Metallic Tin	250 mg
Conc. Sulfuric acid	500 µL
Phenol sulfonic acid	448 µL
Gelatin	10 mg
2-naftol	5 mg
Total Volume	5 mL

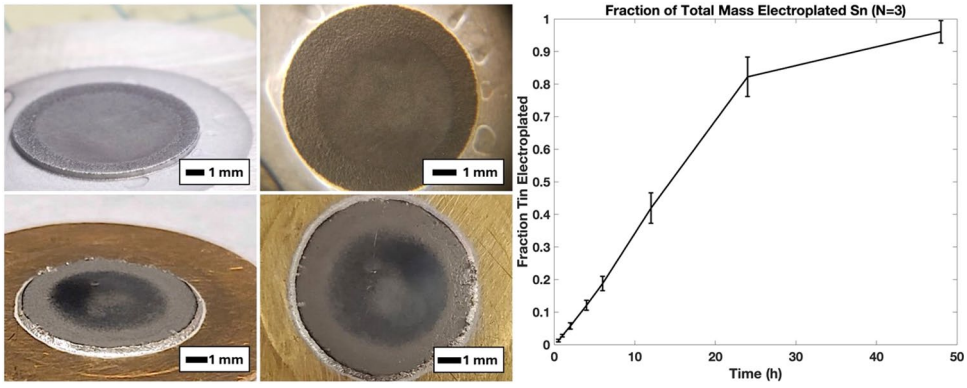

Fig. 1 Two unirradiated, 150 mg (300 mg/cm^2) ^{nat}Sn cyclotron targets plated from non-recycled $SnSO_4$ stock upon silver and gold target backings with surface images shown to the right of their corresponding target image. (right) Sn electrodeposition vs. time. Though Sn electrodeposits upon either silver or gold, gold target backings were employed for productions due to improved labeling performance

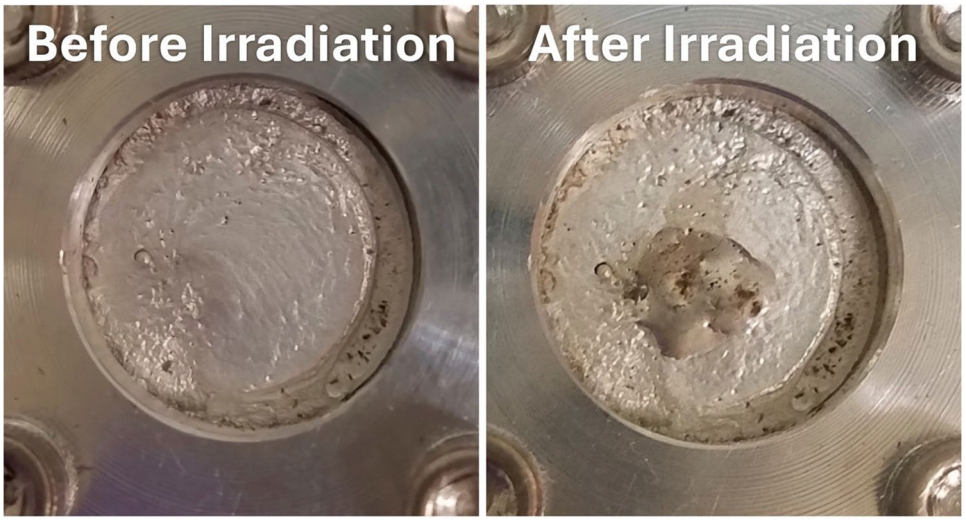

Fig. 2 A representative 290 mg/cm^2 Sn target before (left) and after (right) proton irradiation with 40 μA 16 MeV protons for 6 min

electroplating technique achieves good visual uniformity and thicknesses of >400 mg deposited Sn in an exposed surface area of 0.5 cm^2 (8 mm diameter, ~800 mg/cm^2), resulting in thick targets that absorb all of the 16 MeV proton or 8 MeV deuteron beam energy. Electrodeposited mass over time in this electroplating system is shown in Fig. 1 with greater than 80% of dissolved tin electroplated within the first 24 h.

Target characterization

We employ direct water cooling to the back of gold target disks. Electroplated Sn targets on gold backings with areal density ~300 mg/cm^2 withstood 16 MeV, 40 μA proton irradiation with physical deformations depicted in Fig. 2. No physical deformations were observed over the dozens of 16 MeV, 35 μA proton irradiations for targets with areal density up to 500 mg/cm^2 (>2 h). Targets with >600 mg/cm^2 ^{nat}Sn electroplated onto gold have experienced small deformations at 35 μA of 16 MeV. 100 mg (200 mg/cm^2) ^{nat}Sn targets withstood 40 μA of 8 MeV deuterons with no physical deformations.

Proton irradiation of tin's ten naturally occurring isotopes with 12–16 MeV protons produces a cocktail of antimony, tin, and indium radioisotopes. The measured yields of these residuals are presented in Fig. 3 with EOB physical yields of relevant radioantimony isotopes and varied production parameters. Tabulated presentation of measured EOB physical yields are reported within the supplementary information (Table S1). Antimony-125 was never observed, and when using isotopically enriched ^{119}Sn targets, ^{124}Sb was also not observed. When a radioisotope was not observed, limits of detection (LODs) are reported instead.

Bombarding ^{nat}Sn with 16 MeV protons produces the greatest quantity of radioisotopic impurities when considering the radionuclidic purity of two antimony radioisotopes with greatest medical interest (Figs. 4) – ^{119}Sb and ^{117}Sb. When considering ^{119}Sb, thick ^{nat}Sn targets produced 29.8 ± 3.0 MBq/μAh at a radionuclidic purity of 5.6% ± 0.6% at EOB using 16 MeV protons and 1.55 ± 0.67 MBq/μAh ^{119}Sb at 6% ± 2% radionuclidic purity at EOB using 8 MeV deuterons. The highest purity of ^{117}Sb (92.36% ± 2.00% at EOB) with the lowest contribution from higher dose, longer lived radioisotopic impurities (0.06% ± 0.04% ^{120m}Sb, 0.48% ± 0.26% ^{122}Sb, and 0.07% ± 0.01% ^{124}Sb at EOB) is produced via deuteron bombardment of ^{nat}Sn (isotopically enriched ^{116}Sn or ^{117}Sn was not available for this work). Deuteron bombardment of ^{nat}Sn produces less longer-lived contaminants compared to proton irradiation (~10-fold less ^{122}Sb and ~100-fold less ^{120m}Sb), facilitating pre-clinical imaging in vivo applications.

Figure 5 includes representative HPGe spectra from irradiated, undissolved targets irradiated with protons and deuterons and varied energies. In some of the HPGe spectra, two peaks (133.98 keV, 77.35 keV) are observed from $^{197\ m/g}$Hg produced within the gold target backings. No $^{197\ m/g}$Hg is observed in the radiochemically purified product, and the apparent 511 keV annihilation photons indicate positron emitters, including ^{117}Sb's 1.8% β^+ branching ratio.

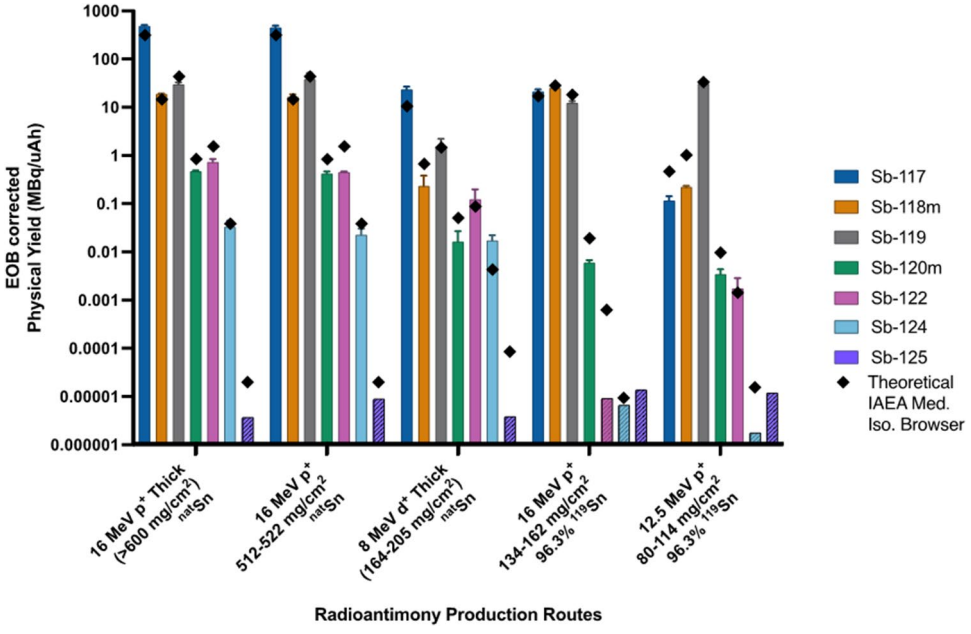

Fig. 3 Comparison of EOB-corrected measured physical and theoretical yields with limits of detection represented as cross-hatched yield bars for each experiment. Theoretical yields calculated using IAEA Medical Isotope Browser (IAEA 2024). All data are $N = 3$ replicates

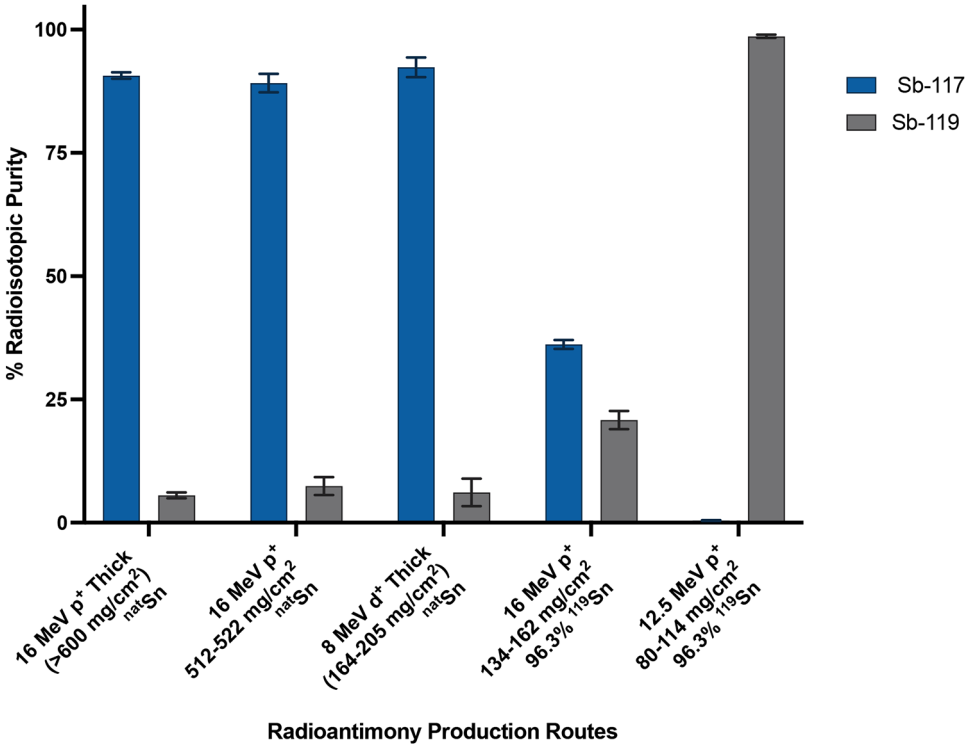

Fig. 4 EOB corrected radionuclidic purity of ^{117}Sb and ^{119}Sb for various characterized production routes. All data are $N = 3$ replicates

Antimony-119 yields were measured directly in a massless source configuration. A representative low energy ^{119}Sb spectra from the CdTe detector is presented within Fig. 6. The characteristic 23.87 keV gamma emission of ^{119}Sb can clearly be seen as a shoulder upon the convolved ~ 25 keV X-ray emissions from many radioantimony contributors. The two overlapping peaks were easily deconvolved into gaussians using Fityk version 1.3.1 (Wojdyr 2010) to separate out the distinct ^{119}Sb photon contribution.

Using 96.3% isotopically enriched ^{119}Sn and 12.5 MeV proton energy, three targets with areal density 80–114 mg/cm^2 produced measured physical yields reported in Table 3 at a radioisotopic purity of 98.9%, decay-corrected to EOB.

Radiochemical isolation of radioantimony from bulk target material

Using HPGe quantification of ^{122}Sb and ^{117m}Sn, elution profiles for both columns are depicted in Fig. 7. The first column in the separation chemistry yields 87.1% ± 3.4% ($N=3$) of loaded radioantimony in 0.75 mL eluted acidic ethanol solution. The second column yields 83.7% ± 4.9% ($N=3$) of loaded radioantimony in 1.39 mL ± 0.05 mL ($N=3$) EtOH, for a combined radiochemical yield of 73.1% ± 6.9% ($N=3$) ^{122}Sb recovery. In the prefilter resin column step, ^{117m}Sn activities were below detection limits and are plotted accordingly.

Apparent molar activity was measured for three productions via deuteron bombardment of ^{nat}Sn targets to be 42.4 ± 25 MBq ^{117}Sb/μmol TREN-CAM (1.14 ± 0.68 mCi/μmol) decay corrected to EOB. First column eluted fractions contain 55 ± 7 μM thiol functional groups, suggesting resin degradation upon contact with 5 M HCl in 48% EtOH. Final eluted fractions from the prefilter resin show sub μg trace metal

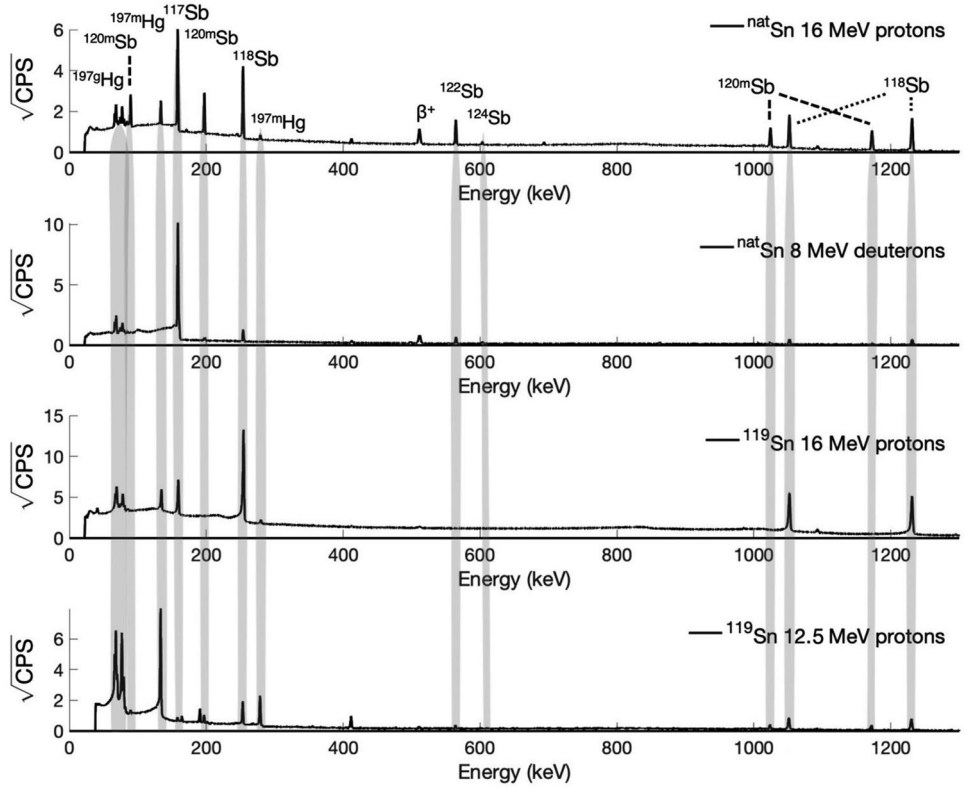

Fig. 5 HPGe gamma spectra of representative irradiated targets depicting significant differences in radioantimony profiles produced via differing production routes. 8 MeV deuteron irradiated target spectrum was collected 1 h post EOB. Proton irradiated target spectra were collected 16 h post EOB

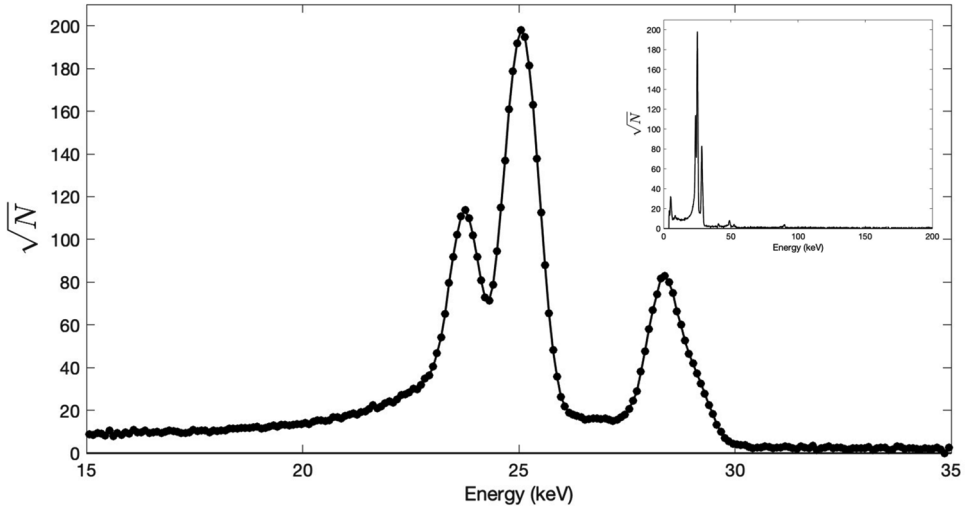

Fig. 6 Low energy X-ray spectrum of purified ^{119}Sb via CdTe detector

content per half mL volume. ICP-OES measurements (Fig. 8) of dissolved target solution before and after target loading of column 1 showed Sn mass loss of 6.3 ± 4.2 mg (N=3). Comparing Sn mass loaded onto the column verse eluted from the column, a separation factor of (6.4 ± 3.7) x 10^3 (N=3) for the first column and (1.7 ± 1.8) x 10^2 (N=3) for the second column, providing a combined separation factor of (6.8 ± 5.5) x 10^5 (N=3). Being

Table 3 Measured EOB corrected physical yields for ^{119}Sb and radioisotopic impurities using 96.3% isotopically enriched ^{119}Sn targets and 12.5 MeV protons

Target Mass (mg/cm^2)	^{119}Sb Yield (MBq/μAh)	^{117}Sb Yield (kBq/μAh)	^{118m}Sb Yield (kBq/μAh)	^{120m}Sb Yield (kBq/μAh)	^{122}Sb Yield (kBq/μAh)	^{124}Sb Yield (kBq/μAh)
80.1	17.5	95.1	210.8	2.5	0.5	< 0.1*
93.8	27.5	110.1	226.1	4.2	2.4	< 0.1*
114.1	34.4	144.8	235.1	3.7	2.4	< 0.1*

* below detection limit of 3 kBq ^{124}Sb

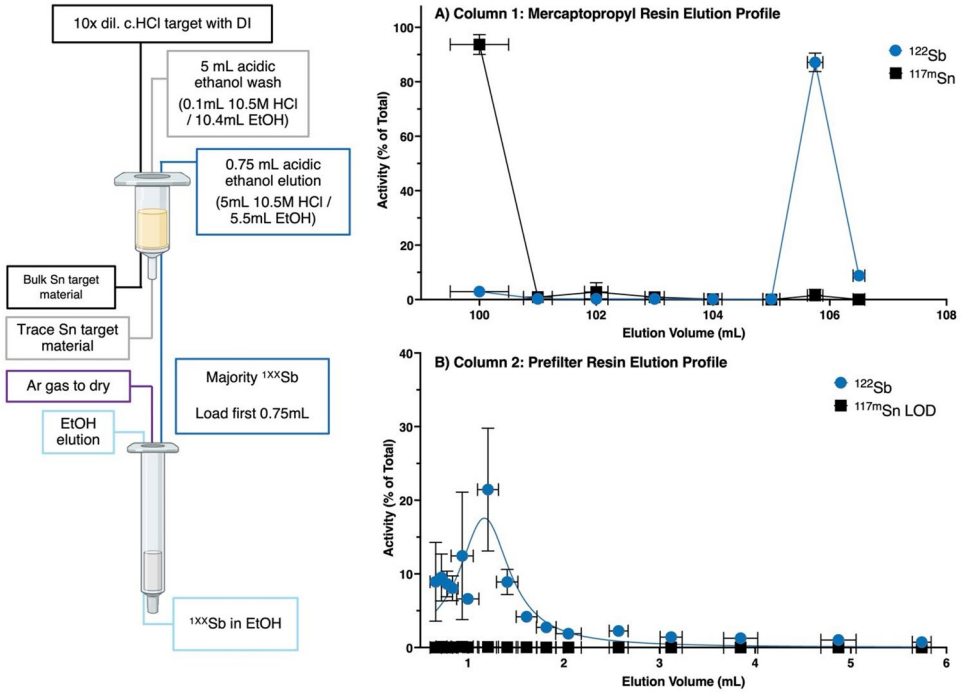

Fig. 7 Scheme showing column chromatography separation to purify ^{1XX}Sb from Sn target material (left). Activity elution profile for (**A**) mercaptopropyl functionalized resin column and (**B**) prefilter resin tracking percent ^{122}Sb and ^{117m}Sn activity. Both elution profiles represent $N = 3$ separations with uncertainty presented as the standard deviation of measurements. (left) Created in BioRender. Olson, A. (2024) http://www.BioRender.com/h73h197

organometallic elements, Sn and Sb have ICP-OES limits of detection on the order of ppm (μg/mL) compared to the ppb limits of detection for transition metals Fe, Cu, Ni, and Co. Measurements of Sb within column 1 and 2 are below observable limits and a measured LOD of 0.1 ppm.

Recycling target material

Iterative recycling of non-irradiated targets was conducted, monitoring the fraction of Sn reclaimed from previously dissolved targets. Comparisons of the time that the dissolved Sn remained in solution before recycling was found to have a significant impact on recycling efficiency, as shown in Fig. 9. Targets with Sn dissolved 8–16 h were recycled with cumulative efficiency 91.3% ± 8.8% (N=12) while targets dissolved > 24 h had cumulative recycling efficiency 66% ± 11% (N=12).

Iterative recycling of irradiated targets (N=3) subjected to first column loading and recycled within 16 h of dissolution provided cumulative recycling efficiency of 86.9% ± 7.8% (N=12) (Fig. 10) with representative images of recycled targets showing the

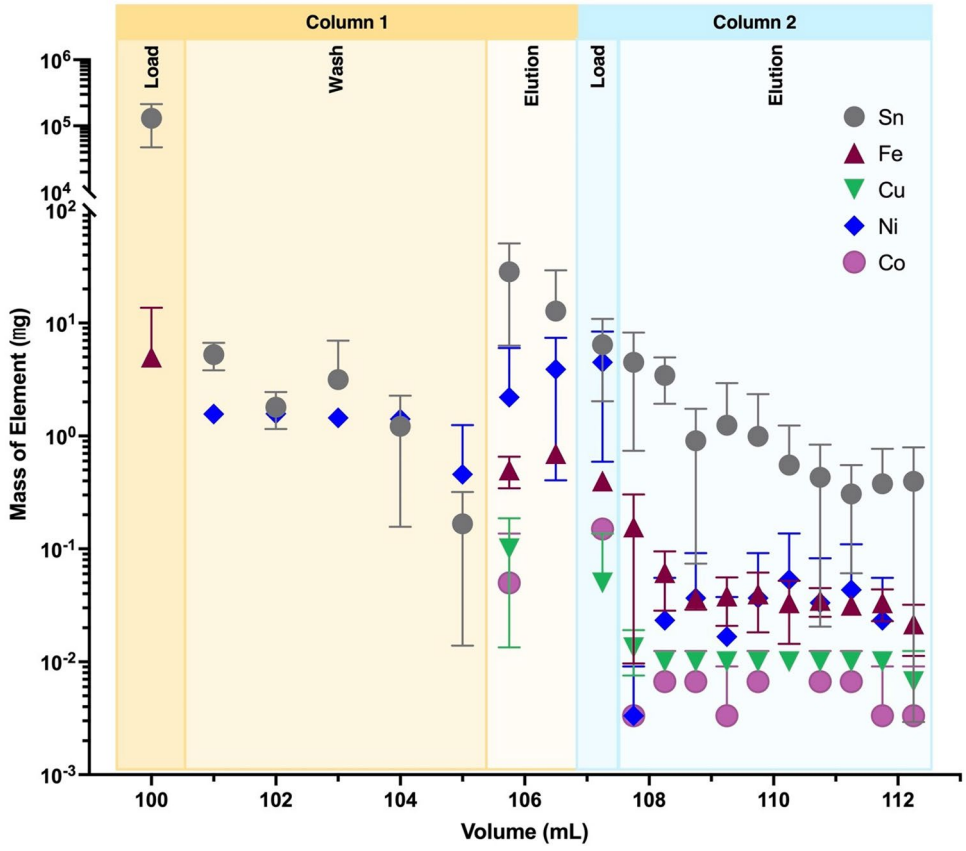

Fig. 8 ICP-OES measured trace metal content in separation chemistry elution fractions. $N = 3$ replicates

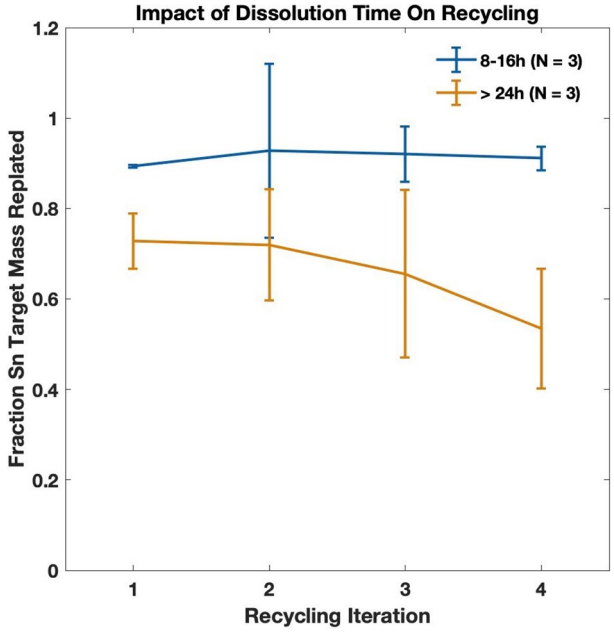

Fig. 9 Non-irradiated target recycling, monitoring the amount of time that the dissolved target was in solution before recycling

capacity to retain metallic Sn quality of electroplates with no observed impact on production yield or beam tolerance. Additionally, irradiated, isotopically enriched ^{119}Sn targets were recycled at an efficiency of 80.2% ± 5.5% (N=6) with 11.6 mg ± 0.8 mg (N=6) lost, potentially to resin loading or oxidation during electroplating process.

Discussion

Antimony-119 is predicted as one of the most promising IC/AE emitting radionuclides for radiopharmaceutical therapy; however, application of this radionuclide is hindered by barriers in production, chemical separation and purification, and radiometal chelation strategies. With measured cross-sections over a barn (Thisgaard and Jensen 2009) and accessibility to low energy proton (<16 MeV) accelerators, production of ^{119}Sb is scalable through (p, n) nuclear reactions on ^{119}Sn, which will require cost effective recycling of expensive enriched material. We report method development and measured production parameters with the intention of decreasing previous ^{119}Sb barriers and increasing availability and accessibility of this radionuclide for greater field exploration and application.

Because of the impact of cross-section on radionuclide production, particle type, particle energy, target isotopic composition, and target thickness are all variables that can be changed and leveraged to modify the resulting radioantimony production profile to desired application needs. Target density and thickness account for the portion of the reaction cross section captured during irradiation process. Thicker targets capture a larger fraction of the cross section than thinner targets, and increasing target thickness

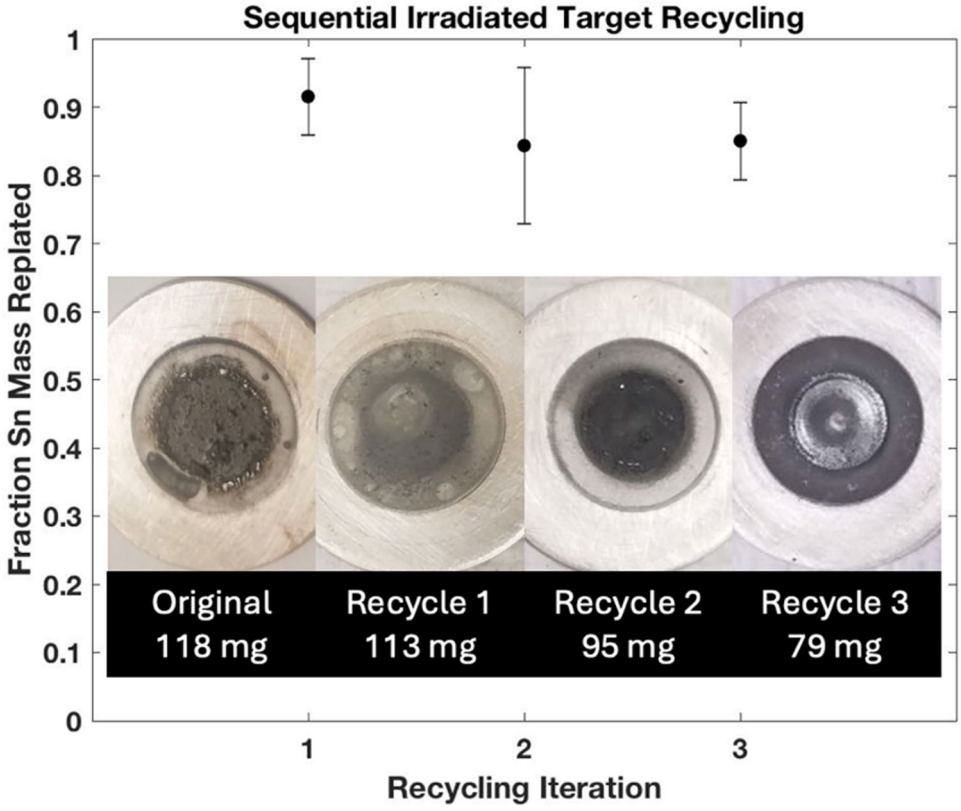

Fig. 10 Iterative recycling of irradiated ^{nat}Sn targets (N=3) processed through chromatographic chemical separation

is one strategy used to increase production yields. Previously, maximum reported electroplated tin cyclotron targets were 15 mg/cm^2 (Thisgaard and Jensen 2009). With ability to electroplate targets > 800 mg/cm^2, which absorb the entirety of the 16 MeV proton energy, target thickness is no longer a barrier limiting production capacity. If one cannot increase target thicknesses, instantaneous physical production yields can be increased by increasing beam current tolerances, increasing duration of irradiation, and implementing slant target geometries so that the beam sees a longer path into the target and beam energy is spread over a larger area, improving target cooling. These strategies are used to compensate for decreased production yields achievable applying these targets at perpendicular geometries.

Charged particle beam tolerance primarily depends on the rates of beam energy deposition and removal from the target. Particle type, particle energy, target composition (electrical and thermal conductance of materials, melting temperature of material) and heat removal strategy bear on these parameters. Considering metals, tin has a low melting temperature of 232 °C (Society 2024), which will contribute to limiting beam current. Using a perpendicular to beam target geometry and direct water cooling upon the target backing, our targets withstand 35 μA 16 MeV proton bombardment, or > 1.1 kW/cm^2 heat dissipation without melting—the highest reported beam tolerance for perpendicular tin target geometries. Using slant target geometries, maximum beam current tolerances of 150 μA on tin have been reported (Thisgaard et al. 2011).

We report measured EOB corrected physical yields for various radioantimony isotopes. In most cases, measured physical yields for ^{117}Sb, ^{118m}Sb, ^{119}Sb, and ^{120m}Sb were comparable to IAEA TENDL predicted values with measured 16 MeV proton yields ranging from 0.5-1.6x IAEA TENDL predicted values and 8 MeV deuteron yields ranging 0.3-2.3x predicted values. Observed differences between measured and predicted values could be due to the beam spot being larger than the target face (Ellison et al. 2020) or TENDL over/underestimating cross section values. Thisgaard measured a ^{119}Sn(p, n)^{119}Sb cross section peak of 1.08 barns ± 0.07 barns at a proton energy of 11.0 MeV ± 0.15 MeV (Thisgaard and Jensen 2009) while the TALYS model presented in TENDL database predicts a cross section of 0.691 barns at 11 MeV (Koning et al. 2019). Yields using thick ^{nat}Sn targets represent maximum production yields (for ^{nat}Sn isotopic enrichment and cyclotron beam spot size) as the entirety of the 16 MeV protons (~ 600 mg/cm^2 Sn) and 8 MeV deuterons (~ 95 mg/cm^2 Sn) are being absorbed. Measured continuous slowing down approximation (CSDA) ranges of protons ((NIST) 1993) modified by deuteron mass ratio allowed calculation of minimum tin mass required to stop particle beams. Tin targets of natural isotopic abundance produced ^{119}Sb with low radioisotopic purity (5.6% via 16 MeV protons, 6% via 8 MeV deuterons), illustrating the requirement for isotopically enriched ^{119}Sn targets for ^{119}Sb production at high radioisotopic purity. Using 96.3% isotopically enriched ^{119}Sn, 12.5 MeV proton energy, and 80–114 mg/cm^2 targets, 26.5 ± 8.5 MBq/μAh ^{119}Sb was produced at a radioisotopic purity of 98.9%, decay-corrected to EOB. Target thicknesses were chosen to minimize use of expensive, enriched material. The largest impurities, ^{117}Sb and ^{118m}Sb, have half-lives significantly shorter than that of ^{119}Sb, and, after the 6 h isolation and radiolabeling of radioantimony, the ^{119}Sb radioisotopic purity increased to > 99.5% by activity. This is illustrated in Fig. 11. A radioisotopic purity of > 99% is maintained for 336 h.

The short half-life of ^{117}Sb (2.80 h) requires timely handling and restricts workflows to <1 d. Also, the low energy emissions of ^{119}Sb (<30 keV) require specialized low energy detection techniques not as widely employed and accessible as HPGe detectors or dose calibrators. Radioisotopes such as ^{120m}Sb and ^{122}Sb have half-lives on the order of days and emit high energy photons that (though easily shielded for radiation worker protection) can be detected with standard gamma detection equipment. For multi-day, radiochemical or targetry development at small scales with tracers, proton bombardment of ^{nat}Sn produces the greatest proportion of these antimony radioisotopes.

We report a radiochemical separation scheme to purify radioantimony from tin in their lower oxidation states (Sb^{3+} and Sn^{2+}) that is compatible with both radioantimony chelation and tin target material recycling. Most reported separation schemes employ Sb^{5+} and Sn^{4+} (Grundmane et al. 2024; Randhawa et al. 2021). Only once has a reported Sb/Sn chemical separation scheme been combined with target recycling (Thisgaard and Jensen 2009). Degradation of column 1 post radioantimony elution could be a future limitation in radioantimony chelation, dependent upon employed chelator. It was not an issue preventing radioantimony complexation with TREN-CAM.

Targets were recycled with high efficiency when target material was dissolved in solution less than 16 h. Plotting via iteration of same target in Fig. 10 shows that recycling efficiency decreases significantly when targets are allowed to sit in the dilute dissolution solution for >24 h before reclamation with final electrolytic solutions turning a dark brown color. We hypothesize loss of tin to oxidation of Sn^{2+}, forming Sn^{4+} which electrodeposits from alkaline as opposed to acidic solutions (He et al. 2008; Møller and Nielsen 2013).

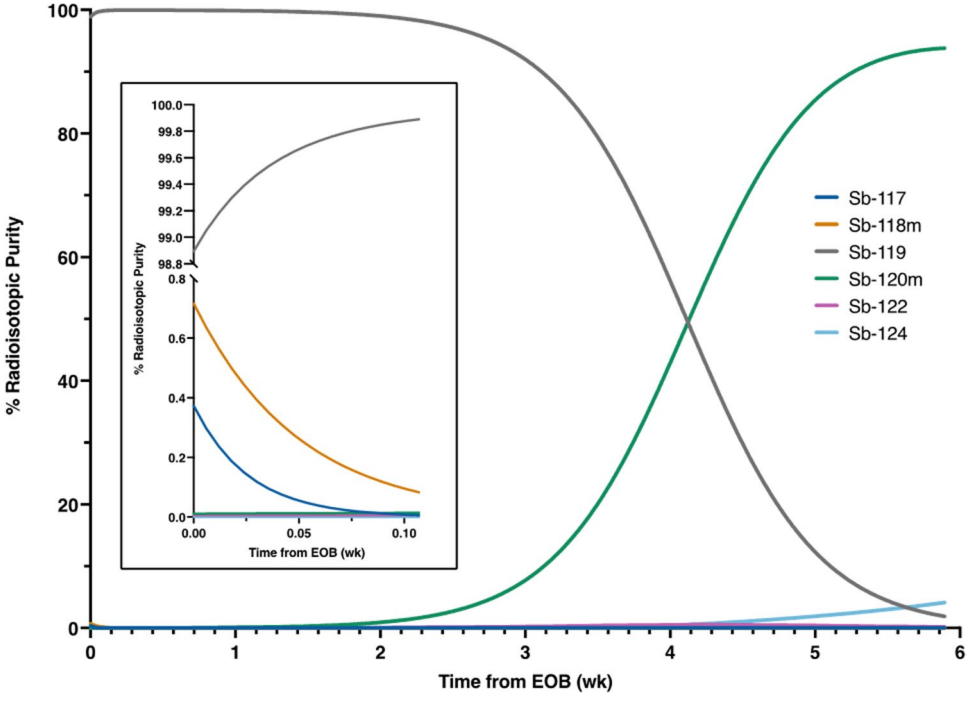

Fig. 11 Radionuclidic purity over time for 12.5 MeV proton irradiation of 96.3% enriched ^{119}Sn targets

Conclusion

We report physical yields for radioantimony isotopes produced with proton and deuteron beams on a small commercial cyclotron. Using an assay technique we developed, ^{119}Sb activity and physical yields were quantified without requiring attenuation correction. Electroplated, sustainably recycled ^{119}Sn targets were irradiated to produce ^{119}Sb in a form and purity suitable for preclinical therapy studies. Gigabecquerel quantity ^{119}Sb was produced with >99.5% radioisotopic purity 6 h post EOB with reasonable cyclotron irradiation parameters (35 μA, 1 h). Our thiol resin separation strategy produced a radiochemical yield of isolated radioantimony of 73.1% ± 6.9% (N=3), without observable ^{117m}Sn contaminant, and provides a Sn separation factor of (6.8 ± 5.5) x 10^5 (N=3). We report the highest AMA for chelated radioantimony among published literature.

Low energy proton and deuteron induced nuclear reactions upon natural and isotopically enriched ^{119}Sn produce a wide range of radioisotopic purity for ^{117}Sb and ^{119}Sb focused productions. When decay correcting to EOB, proton bombardment (16 MeV) of thick natural Sn targets produced greatest ^{117}Sb activities, yet highest purity ^{117}Sb was achieved through deuteron bombardment (8 MeV) of thick ^{nat}Sn. Thin (80–114 mg/cm^2) 96.3% isotopically enriched ^{119}Sn targets achieved the highest purity ^{119}Sb at proton energies of 12.5 MeV, with radioisotopic purity increasing for two weeks post EOB as shorter-lived radioisotopes (^{117}Sb and ^{118m}Sb) decay. Though not explored here, the ^{118}Sn(d, n)^{119}Sb nuclear reaction could provide a cost-effective ^{119}Sb production route, suggested by high ^{119}Sb yields achieved through deuteron bombardment of ^{nat}Sn.

Abbreviations

RPT	Radiopharmaceutical therapy
IC	Internal conversion
AE	Auger electron
EOB	End of bombardment
TREN-CAM	Tris(2-aminoethyl)amine (TREN) catecholamide (CAM)

Supplementary Information

The online version contains supplementary material available at https://doi.org/10.1186/s41181-024-00303-w.

Supplementary Material 1

Acknowledgements

Authors thank Dr. Nikki A. Thiele and Dr. Briana Schrage for synthesizing TREN-CAM.

Author contributions

APO developed methodology, designed experiments, conducted experimental investigation, analyzed data, drafted original manuscript, and reviewed and edited manuscript. FAV conducted non-radioactive experimental investigation, collected ICP-OES measurements, and reviewed manuscript. PAE contributed to method development, experimental design, data analysis, and reviewed and edited manuscript. EA-S contributed to method development, experimental design, and reviewed and edited manuscript. RJN contributed to method development and reviewed and edited manuscript. JCM conducted irradiations and reviewed and edited the manuscript. TEB conducted irradiations, contributed to method development, and reviewed and edited the manuscript. JWE provided project conception, contributed to method development, experimental design, data analysis, and reviewed and edited many versions of the manuscript.

Funding

APO gratefully acknowledges support from NIH F31 Ruth L Kirschstein Predoctoral Individual National Research Service Award F31CA239617. JWE gratefully acknowledges support from the NIH NCI P01CA250972. PAE and JWE acknowledges the Isotope Program, managed by the Office of Science for Isotope R&D and Production, grant number DE-SC0022032. Though in the grant review process funding bodies reviewed research plans, the NIH and DOE were not involved in study design, data collection and analysis, data interpretation, or manuscript writing. The content is solely the responsibility of the authors and does not necessarily represent the official views of the NIH or DOE.

Data availability

Tabulated measured physicals yields are reported within the manuscript and supplementary information. Data is available from the authors upon reasonable request.

Declarations

Ethics approval and consent to participate
Not applicable.

Consent for publication
Not applicable.

Competing interests
A provisional patent for the chelation of radioantimony using TREN-CAM has been filed with APO and JWE as co-authors. The authors have no other competing interests.

Received: 6 September 2024 / Accepted: 10 October 2024
Published online: 22 October 2024

References

(NIST). National Institute of Standards and Technology. PSTAR, ASTAR, ESTAR. ICRU Report 49, International Commission on Radiation Unites and Measurements. 1993.
Bernhardt P, Forssell-aronsson E, Jacobsson L, Skarnemark G. Low-energy electron emitters for targeted radiotherapy of small tumours. Acta Oncol (Madr). 2001;40(5):602–8.
Blachot J. Nuclear data sheets for A = 117. Nucl Data Sheets. 2002;95(3):679–836.
Bodei L, Lewis JS, Zeglis BM. Radiopharmaceutical Therapy. Health Phys. Cham, Switzerland; 2023.
Bolcaen J, Gizawy MA, Terry SYA, Paulo A, Cornelissen B, Korde A, et al. Marshalling the potential of Auger Electron Radiopharmaceutical Therapy. J Nucl Med. 2023;64(9):1344–51.
Eckerman KF, Endo A. MIRD: Radionuclide Data and Decay schemes. 2nd ed. Society of Nuclear Medicine; 2008.
Ellison PA, Olson AP, Barnhart TE, Hoffman SLV, Reilly SW, Makvandi M et al. Improved production of ^{76}Br, ^{77}Br and ^{80m}Br via CoSe cyclotron targets and vertical dry distillation. Nucl Med Biol [Internet]. Elsevier Inc.; 2020;80–81:32–6. https://doi.org/10.1016/j.nucmedbio.2019.09.001
Ellman GL. Tissue sulfhydryl groups. Arch Biochem Biophys. 1959;82:70–7.
Falzone N, Fernández-Varea JM, Flux G, Vallis KA. Monte Carlo evaluation of Auger electron-emitting theranostic radionuclides. J Nucl Med. 2015;56(9):1441–6.
Filosofov D, Kurakina E, Radchenko V. Potent candidates for Targeted Auger Therapy: Production and radiochemical considerations. Nucl Med Biol [Internet]. Elsevier Inc.; 2021;94–95:1–19. https://doi.org/10.1016/j.nucmedbio.2020.12.001
Grundmane A, Radchenko V, Ramogida CF. Chemistry of Antimony in Radiopharmaceutical Developmemnt: unlocking the Theranostic potential of sb isotopes. ChemPlusChem. 2024;(e202400250).
He A, Liu Q, Ivey DG. Electrodeposition of tin: a simple approach. J Mater Sci: Mater Electron. 2008;19(6):553–62.
IAEA. Medical Isotope Browser. 2024.
Joaqui-Joaqui MA, Pandey MK, Bansal A, Raju MVR, Armstrong-Pavlik F, Dundar A, et al. Catechol-based functionalizable ligands for gallium-68 positron emission tomography imaging. Inorg Chem. 2020;59(17):12025–38.
Koller AJ, Glaser O, DeLuca MC, Motz RN, Amason EK, Carbo-Bague I et al. Off-label use of the Siderophore Enterobactin enables targeted imaging of Cancer with Radioactive Ti (IV). Angew Chem. 2024;136(18).
Koning A, Rochman DA, Sublet JC, Dzysiuk NR, Fleming MJ, van der Mark SC. TENDL: Complete Nuclear Data Library for innovative Nuclear Science and Technology. Nucl Data Sheets. 2019;155:1–55.
Kostelnik TI, Olson AP, Grundmane A, Ellison PA, Mynerich J, Chen S, et al. Production and Radiochemistry of Antimony-120m: efforts toward Auger Electron. Nucl Med Biol. 2023;108352:122–3.
Ku A, Facca VJ, Cai Z, Reilly RM. Auger electrons for cancer therapy – a review. EJNMMI Radiopharm Chem EJNMMI Radiopharmacy Chem; 2019;4(1).
Møller P, Nielsen LP. Advanced Surface Technology. 2nd ed. 2013.
Olson AP, Ma L, Feng Y, Najafi Khosroshahi F, Kelley SP, Aluicio-Sarduy E, et al. A third generation potentially bifunctional Trithiol Chelate, its ^{nat,1XX}Sb(III) complex, and selective chelation of Radioantimony (^{119}Sb) from its Sn Target. Inorg Chem. 2021;60(20):15223–32.
Olson AP, Schrage BS, Islam MF, Fletcher LS, Verich FA, Dierolf MA et al. Establishing the stable chelation of Radioantimony(V) for targeted Auger Theranostics. Submitted Angewandte Chemie - Int Ed September *30th*, 2024.
Otuka N, Takács S. Definitions of radioisotope thick target yields. Radiochim Acta. 2015;103(1):1–6.
Randhawa P, Olson AP, Chen S, Gower-Fry KL, Hoehr C, Engle JW, et al. Meitner-Auger Electron emitters for targeted Radionuclide Therapy: Mercury-197m/g and Antimony-119. Curr Radiopharm. 2021;14(4):394–419.
Riddles PW, Blakeley RL, Zerner B. Reassessment of Ellman's reagent. Methods Enzymol. 1983;91(C):49–60.
Society RC. Periodic Table. RCS.org. 2024.
Symochko DM, Browne E, Tuli JK. Nuclear Data sheets for a = 119. Nucl Data Sheets. 2009;110(11):2945–3105.
Thisgaard H, Jensen M. 119Sb - A potent Auger emitter for targeted radionuclide therapy. Med Phys. 2008;35(9):3839–46.
Thisgaard H, Jensen M. Production of the Auger emitter ^{119}Sb for targeted radionuclide therapy using a small PET-cyclotron. Appl Radiat Isot. 2009;67(1):34–8.
Thisgaard H, Jensen M, Elema DR. Medium to large scale radioisotope production for targeted radiotherapy using a small PET cyclotron. Applied Radiation and Isotopes [Internet]. Elsevier; 2011;69(1):1–7. https://doi.org/10.1016/j.apradiso.2010.07.019
Wojdyr M, Fityk. A general-purpose peak fitting program. J Appl Crystallogr. 2010;43(5 PART 1):1126–8.

Publisher's note